Monitoring of Denaturation Processes in Aged Beef Loin by Fourier Transform Infrared Microspectroscopy

C. Kirschner, R. Ofstad, H.-J. Skarpeid, V. Høst, and A. Kohler*

MATFORSK, Norwegian Food Research Institute, Osloveien 1, N-1430 Ås, Norway

We present the results of a Fourier transform infrared (FT-IR) microspectroscopic study using conventional FT-IR microscopy and FT-IR imaging to detect the denaturation process during four different heating temperatures (raw, 45, 60, and 70 °C) spatially resolved in bovine cryosections from *longissimus dorsi* muscle. FT-IR imaging, employing a focal plane array detector, which allowed the simultaneous collection of spectra at 4096 pixels, enabled the investigation of the heat-induced changes in the two major meat constituents, i.e., myofibrillar and connective tissue proteins, spatially resolved. The infrared spectra of both compounds revealed that the major spectral changes involved an increase in β-sheet and a decrease in α-helical structures, which appeared to be much more pronounced for the myofibers than for the connective tissue. These conformational changes could be correlated to the denaturation of the major meat proteins, such as myosin, actin, and collagen.

KEYWORDS: FT-IR microscopy; FT-IR imaging; thermal denaturation; myosin; actin; collagen; partial least squares regression; principal component analysis

1. INTRODUCTION

Texture and functionality of meat from mammalian muscle depend on its myofibrillar and connective tissue proteins (*1*). Studies on both compounds during aging of meat, which is used to increase tenderness, have shown that both components affect the final quality of meat (*2, 3*). Heating is one of the most important steps in the processing of muscle foods. Therefore, the study of the thermal behavior of meat myofibrillar and connective tissue proteins is an important task in determining and predicting the final quality of meat products. Different techniques such as differential scanning calorimetry (DSC), scanning electron microscopy, and Warner Bratzler shear force measurements have been used to study the thermal properties of proteins in muscle tissue, as well as of isolated muscle proteins (*4−8*). However, all of these methods have in common that the information provided is restricted to a few components of the meat sample only.

The application of vibrational spectroscopic methods, such as infrared (IR) and Raman spectroscopy, offers a potential alternative in the field of meat research, since these techniques enable the monitoring of changes in all biomolecules present in the sample in situ. Meat is, like most complex biological materials, spatially and chemically heterogeneous. The use of Fourier transform (FT)-IR microspectroscopy (*9*), as a combination of spectroscopy and microscopy, and more recently FT-IR microspectroscopic imaging (*10*), employing FPA (focal plane array) detectors, provides a tool to simultaneously investigate both of these properties, thus improving the ability to better understand the molecular composition and morphology of such complex tissues. Measurements using the single pixel detector are referred to as FT-IR microspectroscopy, whereas measurements employing the FPA detector are referred to as FT-IR imaging in the following. The use of FPA detectors (employing 64×64 pixels) instead of a single pixel detector affords temporal advantage over mapping experiments, a better spatial resolution, and superior image fidelity (*11*).

While FT-IR microspectroscopy is already becoming a useful analytical tool mainly in biomedical sciences, e.g., for tissue characterization by studying specifically the molecular alterations associated with different diseases, such as cancer and TSE (transmissible spongiform encephalopathies) (*12, 13*), the FT-IR imaging technique remains in general underutilized due to the costs of the FPA detectors. Only a few applications of FT-IR imaging for food analysis have been described so far, such as the characterization of in situ plant tissue (*14, 15*).

The purpose of this study was to evaluate the potency of FT-IR microspectroscopy, with special emphasis on FPA detection, for monitoring denaturation processes in connective tissue and single muscle fibers. Another focus was to optimize methodology for use of complex IR images (comprising $64 \times 64 = 4096$ spectra, i.e., one spectrum corresponds to one pixel) to monitor denaturation processes.

2. MATERIALS AND METHODS

2.1. Sample Preparation. *Longissimus dorsi* muscles from four Norwegian Red Cattle obtained from a local slaughterhouse were used. The muscles were excised from the carcasses 45 min postmortem and stored at 12 °C for 26 h to avoid cold-shortening. From each of the four muscles (animals), four cross-sectional slices of 3.5 cm were cut transversally to the fiber direction from the same location in the muscle. The slices were packed in polyamide/polyethylene bags under slight

---

* To whom correspondence should be addressed. Tel: +47-64970240. Fax: +47-64970333. E-mail: achim.kohler@matforsk.no.

Denaturation Processes in Aged Beef Loin

J. Agric. Food Chem., Vol. 52, No. 12, 2004 **3921**

vacuum and aged at 4 °C for 7 days according to the described procedure for meat used before physical measurements (*16*). For heat treatment, three of the individual vacuum-packed samples for each muscle (animal) were suspended in a preheated water bath at 45, 60, and 70 °C for 50 min while one raw sample was kept as the control sample. Further cooking was then inhibited by placing the samples in running cold tap water for 50 min.

Muscle blocks (5 mm × 5 mm × 2 mm) excised from the middle of the raw or heated meat slices were embedded in O.C.T. compound (Tissue-Tek, Electron Microscopy Sciences, Hatfiles, U.S.A.), immediately frozen in liquid N_2, and stored at −70 °C prior to sectioning. The samples were sectioned (at −22 °C) transversally to the fiber direction. A cryostat (Leica CM 3050 S, Nussloch, Germany) was used, and 8 μm thick sections were prepared and thaw-mounted on IR transparent 2 mm thick CaF_2 slides for FT-IR microscopic measurements. The sections for IR microscopy were finally freeze-dried in an in-house build lyophilizer at room temperature for 6 min applying a vacuum of 0.06−0.08 mbar and stored under dry conditions.

The following sets of spectra were acquired. (i) For the analysis of spectral variation in one animal and from animal to animal of raw not-aged material, spectra of myofibers of cryosections from two different locations (obtained from either end of the *longissimus dorsi* muscle), from two different blocks, a and b, and from two different animals, A and B, were acquired, resulting in 40 spectra in total.

(ii) For the analysis of changes in FT-IR spectra of myofibers due to heat treatment, FT-IR spectra were recorded from five randomly selected myofibers on sections from one muscle block of each of the four animals resulting in 20 spectra for each treatment and 80 spectra in total (spectra of raw material that was aged for 7 days included).

(iii) For the analysis of changes in FT-IR microscopic images and connective tissue spectra, FT-IR images from areas containing connective tissue and myofibers were acquired from three randomly selected areas on sections of one muscle block of each animal and each treatment, resulting in 12 spectra per treatment and 48 spectra in total (spectra of raw material that was aged for 7 days included). The spectra were extracted from the images as described in section 2.2.2. It is important to note that for the investigation of the heat treatment process only the aged raw samples are compared to the heat-treated samples.

2.2. IR Data Collection and Evaluation. *2.2.1. FT-IR Microspectroscopy.* We used an IR microscope (IRscope II) coupled to an Equinox 55 FT-IR spectrometer (both Bruker Optics, Germany) to measure the tissue sections. The microscope was equipped with a computer-controlled *x,y* stage. The Bruker system was controlled with an IBM compatible PC running OPUS-NT software, version 4.0. IR spectra were collected from single myofibers (30−60 μm in diameter depending on the heat treatment) in transmission mode from 4000 to 700 cm^{-1} with a spectral resolution of 6 cm^{-1} using a mercury−cadmium−tellurium detector. For each spectrum, 256 interferograms were coadded and averaged. The microscope, which was sealed using a specially designed box, and the spectrometer were purged with dry air to reduce spectral contributions from water vapor and CO_2. A background spectrum of the CaF_2 substrate was recorded before each sample measurement in order to account for variations in water vapor and CO_2 level.

2.2.2. FT-IR Microspectroscopic Imaging. An FT-IR imaging system, employing a FPA detector with 64 × 64 pixels, was used to measure sample areas containing connective tissue and myofibers. Absorbance spectra were recorded using step scan mode in the range from 3800 to 900 cm^{-1} with a spectral resolution of 8 cm^{-1}. Spectra were apodized (*17*), i.e., mathematically smoothed, by applying a Blackmann−Harris three term apodization function along with a zero-filling function of 2. Analysis of the IR images was performed with in-house developed software in C++. The Microsoft C++ Developer Studio was used to create Dynamic Link Libraries that were linked to Dynamic Imager, an image analysis developer platform (Ceetron ASA, Trondheim, Norway). This software enabled us to extract spectra from defined tissue structure, e.g., connective tissue from the complex IR images comprising 4096 spectra.

2.2.3. Quality of the Spectra. The general strategy for data evaluation was identical for the applied spectroscopic techniques. The first step of data analysis included a quality test of the raw data, e.g., check for water vapor, sample thickness, and signal-to-noise ratio (S/N) (see ref *18* for more details). Spectra that have passed this quality test were converted to 1st derivatives applying a nine point Savitzky−Golay filter to enhance the resolution of superimposed bands and to minimize problems from unavoidable baseline shifts and subsequently vector-normalized to account for different amounts of biomass as described elsewhere (*19*).

The spectra acquired with the FPA detector required a quality test implying lower quality parameters than for the spectra recorded with the single element detector. This is due to a lower S/N ratio of the FPA images and also to a poorer quality of the connective tissue spectra in general. Spectra acquired with the FPA detector were considered to have passed the quality test if they met the following criteria: noise less than 2×10^{-3}, amide I S/N ratio greater than 10, S/N ratio of the mixed spectral region (1500−1200 cm^{-1}) greater than 4, water (vapor) of less than 8×10^{-4}, amide I S/W (signal-to-water) ratio greater than 40, and S/W ratio of the mixed spectral region greater than 10. For the FPA images displayed in **Figure 10a−d**, 3560, 3247, 1537, and 1242 spectra (out of 4096 total spectra per image), respectively, met the criteria listed.

The quality test of the spectra recorded with the single element detector was carried out with OPUS-NT, whereas the quality test of the FPA images was performed with in-house developed software as described above.

2.2.4. Multivariate Analyses. Multivariate statistical analyses, i.e., principal component analysis (PCA) and partial least squares regression (PLSR) of the data, were performed using the Unscrambler software package (version 7.6; Camo ASA). Additional analysis of IR spectral data (calculation of derivatives, normalization, etc.) was performed using the OPUS-NT software version 4.0 (Bruker Optics).

For the calculation of total spectral intensities for IR images, we used the chemometric preprocessing method extended multiplicative scatter correction (EMSC) (*20*). The idea of EMSC is to write every spectrum as

$$\mathbf{z}_i = a_i\mathbf{1} + b_i\mathbf{m} + d_i\tilde{\nu} + e_i\tilde{\nu}^2 + \epsilon_i \tag{1}$$

a linear combination of a baseline shift a_i, a multiplicative effect b_i times a reference spectrum $\mathbf{m}$, and wavenumber dependent effects d_i and e_i. The vector $\mathbf{1}$ is defined as a flat baseline row vector $\mathbf{1} = [1,1,1, ... 1]$ and is introduced for formality reasons. The vectors $\tilde{\nu}$ and $\tilde{\nu}^2$ model linear and quadratic wavenumber-dependent effects, respectively. The vector ϵ_i contains the unmodeled residuals. The EMSC parameters a_i, b_i, d_i, and e_i are estimated by PLS as described in detail in ref *20*. The parameter b_i is basically determined by the thickness of the sample used for FT-IR microscopy and can therefore be used as a measure of total spectral intensity. The software for EMSC is written in Matlab (The MathWorks Inc., Natick, United States) and was provided by courtesy of Harald Martens (*20*).

3. RESULTS AND DISCUSSION

3.1. FT-IR Microspectroscopy. Figure 1 displays a typical spectrum of a randomly selected myofiber (fiber type not identified) obtained from a raw *longissimus dorsi* cryosection in the spectral region from 4000 to 1000 cm^{-1}. The most prominent band in the myofiber spectrum is the amide I band, which occurs in the region between 1700 and 1600 cm^{-1}. This band reflects an almost pure vibrational character, since it represents primarily the carbonyl stretching vibration of the amide bonds (80%) in the protein backbone with a minor contribution from the C−N stretching and N−H bending vibrations. Of all of the amide bands, of which there exist nine, the amide I band was found to be the most useful for the analysis of secondary structure of proteins because of its sensitivity to hydrogen-bonding pattern, dipole−dipole interaction, and the geometry of the polypeptide backbone (*21−23*). Typically, the amide I band consists of overlapping component bands, which
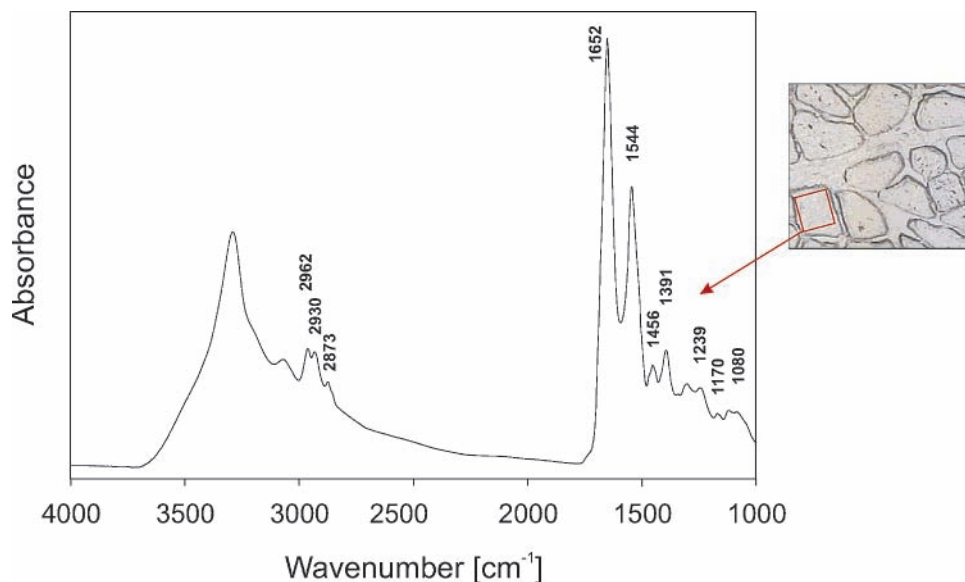
Figure 1. Typical IR spectrum obtained from a single myofiber of a raw *longissimus dorsi* muscle tissue section. Major absorption bands are indicated. For more specific band assignments, see also **Table 1**.

occur as a result of the secondary structures present in such molecules, such as α-helices, β-sheets, turns, and irregular structures.

3.1.1. Multivariate Analysis of Myofibril Spectra from Different Samples and Different Locations within One Sample. To estimate the variance within one raw muscle of one animal, we used data set 1 as described in the Materials and Methods section (2.1) but only for one animal, i.e., including 20 spectra in total. Then, PCA analysis was applied, since it is a well-known technique for the extraction and interpretation of systematic variance in multidimensional data sets by means of a small number of noncorrelated variables (*24*). PCA finds directions in the data that explain most of the variance. These new axes are linear combinations of the original ones and are orthogonal and ordered with respect to the amount of explained variance. After PCA, the first few principal components capture the main variance and remove the random variation, i.e., noise. In many cases, it is enough to look at the scores of the first two principal components.

Figure 2 shows the score plot of the first and the second principal component based on 20 myofiber spectra (1780–1000 cm^{-1}) corresponding to the sections obtained from two different locations (1 or 2) and two different blocks (a or b) from each location within the sample. The score plot, a projection of the original data onto the principal components, allows a visualization of the clustering of the spectra. The score plot of PC1 vs PC2 displays a distinct clustering according to the sampling (**Figure 2**) with the spectra obtained from five different myofibers of each section being grouped together. PC1 separates the two different locations, whereas PC2 separates the two different blocks from each location.

In the next step, the variance of IR spectra (1780–1000 cm^{-1}) obtained from different animals was investigated. PCA analysis was applied to the whole data set 1 as described in the Materials and Methods section (2.1), comprising a total of 40 spectra. The score plot is displayed in **Figure 3** where no clear grouping can be observed. These findings demonstrate that the variation between FT-IR microcopy spectra from different locations of the same samples is comparable to the variation of the FT-IR spectra obtained from different animals.

3.1.2. Multivariate Analysis of the Myofiber Spectra from the Heat Denaturation. PCA analysis was used in order to estimate
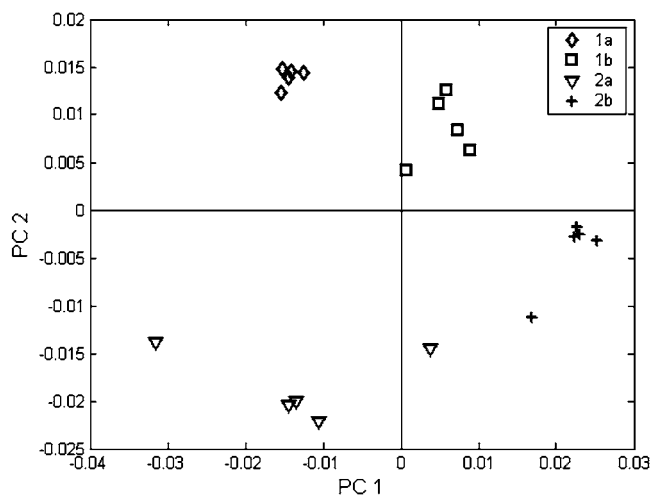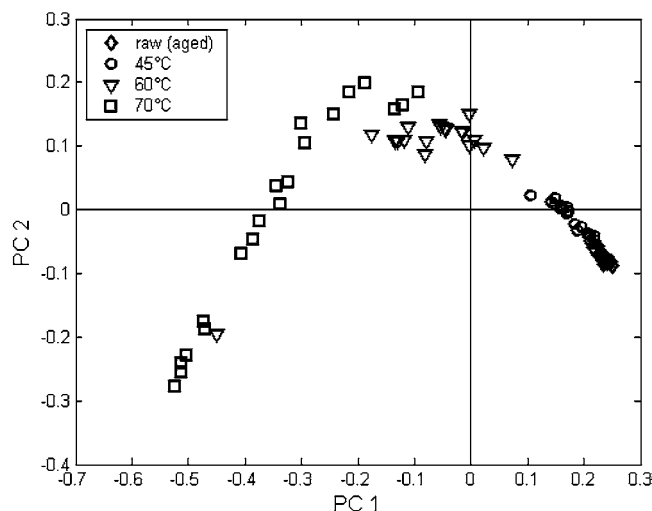

Figure 2. Score plot of the IR spectra obtained from myofibers from PCA of one sample. The numbers 1 and 2 correspond to two different locations within the sample, and the letters a and b correspond to two different blocks from the same location. Five different myofibers were measured per location and block resulting in a total of 20 spectra, which were included in the regression. PCA was performed using the spectral region from 1780 to 1000 cm^{-1}. The explained variances in X by PC1 and PC2 were 42 and 26%, respectively.

the variance of the myofiber spectra (1700–1600 cm^{-1}) from the heat denaturation of all four animals. The score plot is displayed in **Figure 4** showing four clusters according to the four different temperatures, i.e., raw (aged for 7 days), 45, 60, and 70 °C. Interestingly, the clusters become significantly more widespread with higher temperatures, indicating a higher variation of the myofiber spectra upon increasing denaturation. The myofiber spectra of the samples heat-treated at 70 °C exhibit the highest variation, which might be due to the fact that 70 °C represents a transition temperature. The degree of aging of meat has been shown to effect the thermal stability of tissue structures (*1*). The rate of postmortem degradation depends on the fiber type (*25*). In fish also, large variation in the postmortem structural alterations among the white fibers (type IIB) has been reported (*26*). The variation of the myofiber spectra at 70 °C may therefore reflect different degrees of postmortem degrada-

Denaturation Processes in Aged Beef Loin

*J. Agric. Food Chem.,* Vol. 52, No. 12, 2004 **3923**
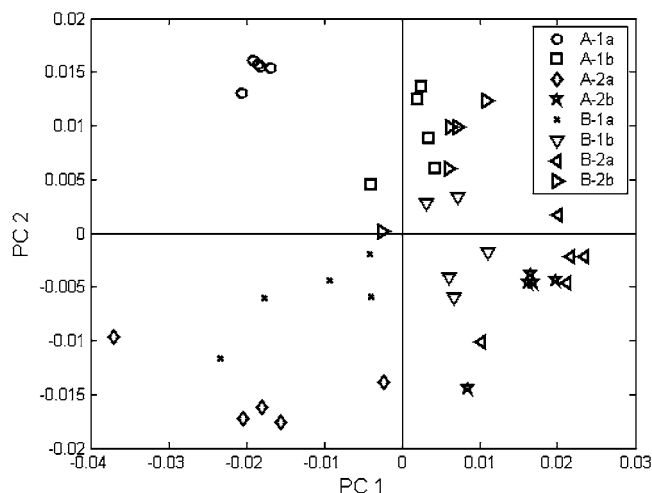
Figure 3. Score plot of the IR spectra obtained from myofibers from PCA of two different samples. The letters A and B correspond to the two different samples. Again, 1 and 2 correspond to two different locations within the same sample, and a and b correspond to two different blocks from the same location. Five different myofibers were measured per location and block resulting in a total of 40 spectra, which were included in the regression. PCA was performed using the spectral region from 1780 to 1000 cm^{-1}. The explained variances in X by PC1 and PC2 were 38 and 17%, respectively.

Figure 4. Score plot of the IR spectra obtained from myofibers from PCA of all four samples during the heat treatment. Five different myofibers were measured per sample and temperature resulting in a total of 80 spectra, which were included in the regression. PCA was performed using the amide I region from 1700 to 1600 cm^{-1}. The explained variances in X by PC1 and PC2 were 82 and 17%, respectively.

tion in the myofibrillar proteins between the different muscle cells. In addition, the score plot shows that the denaturation process is very well-described by the first and second principal component, since the scores of the first and the second principal component separate objects referring to different temperatures very well. The scores are showing a continuous process up to 60 °C, which reflects a progressing denaturation. However, upon 70 °C, a sharp bend in the otherwise continuous score plot can be observed indicating that the IR spectra reflect a chemical change, which is different from the change occurring between raw, 45, and 60 °C. The reason for that approximately one-third of the samples is still within the linear range may again be explained by the fact that 70 °C represents a transition temperature and that the variation in the samples heat-treated
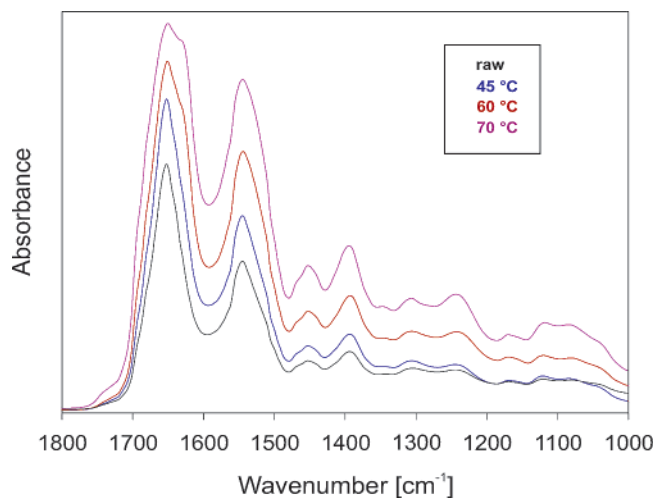
Figure 5. IR spectra displayed over the frequency range 1800–1000 cm^{-1} obtained from myofibers from bovine *longissimus dorsi* muscle heat-treated at four different temperatures: raw, 45, 60, and 70 °C (from bottom to top).

with 70 °C is larger than for the other temperatures. These findings will have to be investigated in further studies, which are currently underway.

3.1.3. Changes in the Myofibril Spectra upon Heat Treatment. The temperatures for heat treatment (45, 60, and 70 °C) were chosen according to the denaturation behavior of the main muscle components, the myofibrillar and connective tissue proteins, i.e., actin, myosin, and collagen, which will be explained in the following in more detail.

During cooking/heating, the proteins within and around the myofiber progressively denature as they reach characteristic temperatures. On the basis of Warner−Bratzler shear force measurements and DSC, it is well-known that the denaturation process upon heating is reflected in changes in the toughness of beef muscle (*2, 27*). According to these studies, meat toughness is found to increase in two distinct phases. The first increase in toughness between 40 and 55 °C is most likely due to the heat denaturation of myofibrillar proteins, especially myosin. This is followed by a decrease in toughness between 50 and 65 °C, which can be attributed to thermal structural changes of the connective tissue resulting in the shrinkage of endomysial and perimysial collagens. The second increase in toughness at temperatures above 65 °C can be subsequently explained by denaturation of actin and sarcoplasmic proteins.

Figure 5 shows typical FT-IR spectra from myofiber tissue heat-treated at four different temperatures, i.e., raw, 45, 60, and 70 °C. Comparison of the spectra reveals that the major changes upon heat treatment occur in the amide I region exhibiting two well-defined shoulders at 1630 and 1695 cm^{-1} at higher temperatures. To resolve the overlapping amide I band components and hence the secondary structure of the myofibrillar proteins, derivatization was applied.

The second derivatives of the same myofiber spectra as in **Figure 5** are shown in **Figure 6** in the spectral region between 1750 and 1500 cm^{-1}. Second derivatives were calculated to enhance resolution of the spectral bands and to minimize baseline variations in the spectra. The second derivative spectra reveal significant spectral alterations in the amide I region during the heat-induced denaturation with more marked changes at higher temperatures. With increasing temperature, the bands at 1630 and 1695 cm^{-1} show significant higher band intensity. These bands have been described to be diagnostic for antiparallel *β*-sheets (*28*). This split amide I mode arises from transition
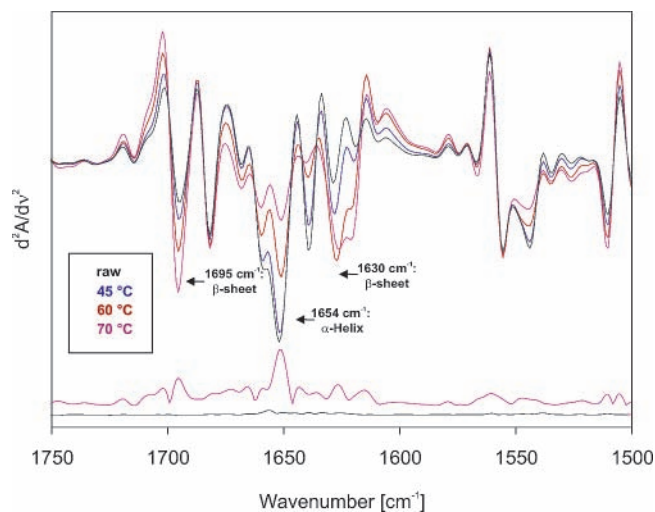
Figure 6. Normalized second derivatives of average spectra each obtained from single spectra of five myofibers from bovine *longissimus dorsi* muscle heat-treated at four different temperatures, i.e., raw, 45, 60, and 70 °C (from bottom to top) are displayed over the frequency range 1750–1500 cm^{-1} (amide I and II region). The SDs for the raw and the 70 °C heat-treated muscle are shown in the bottom.

dipole coupling between carbonyl oscillators in the β-core (*29, 30*). In addition, a slight shift can be observed in the low frequency β-component (1630 cm^{-1}) at 60 and 70 °C, respectively. Such an increase between the low and the high frequency β-component has been described as characteristic for thermally aggregated proteins indicating intermolecular β-sheet structure with very strong hydrogen bonds in comparison to that observed from β-sheets in native proteins (*21*). However, the band at 1654 cm^{-1}, which can be assigned to α-helical structures, shows in contrast reduced band intensity upon increasing temperature indicating that the content in α-helical structures is reduced during heat denaturation. It should be noted that the standard deviations (SDs) of the myofiber spectra (see bottom of **Figure 6**) of the raw sample are significantly smaller than the SDs of the myofiber spectra of the muscle sample heat-treated at 70 °C. As was already found with the score plot of the heat-treated samples in **Figure 4**, the average spectra of the 70 °C heat-treated samples differ considerably. Nevertheless, the observed spectral alterations during the heat denaturation are significant as compared to the SDs.

3.2. FPA Detection. FPA detection was used to monitor the denaturation process in tissue areas containing myofibers as well as connective tissue.

3.2.1. Changes in the Connective Tissue Spectra upon Heat Treatment. Spectra from connective tissue were extracted from the IR images by means of in-house developed software. The quality of the connective tissue spectra was in general poorer than for the myofibers due to lower amounts of biomass and the lower signal-to-noise (S/N) ratio of the FPA measurements, which can be attributed to the larger noise than that commonly encountered in single element detectors (see for more details refs *31* and *32*). Average spectra from a total of 30 spectra for each sample were calculated. **Figure 7** shows the average FT-IR spectra from connective tissue heat-treated at four different temperatures, i.e., raw, 45, 60, and 70 °C. The spectrum of the untreated (raw) connective tissue (bottom spectrum) reveals vibrational modes, which can be assigned as follows: 1662 and 1638 cm^{-1}, amide I; 1553 cm^{-1}, amide II; 1456 and 1403 cm^{-1}, deformation bands of methyl groups; and 1342, 1286, 1240, and 1205 cm^{-1}, amide III and methylene wagging vibrations
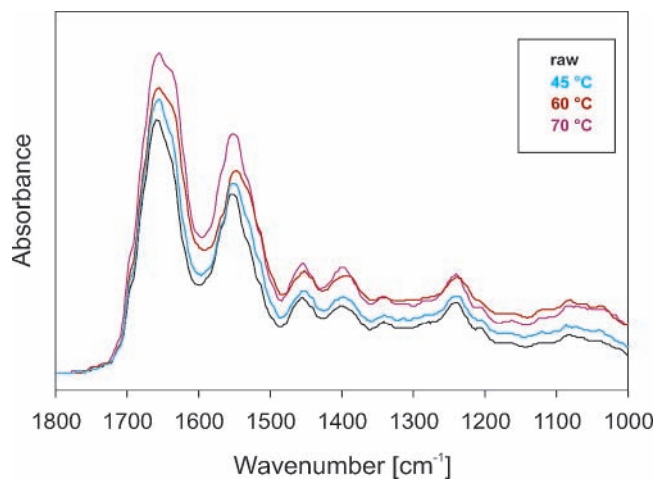
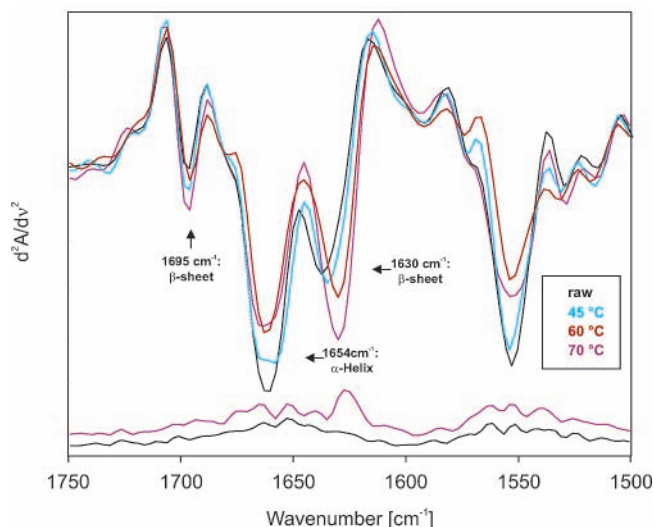

Figure 7. IR spectra displayed over the frequency range 1800–1000 cm^{-1} obtained from connective tissue from bovine *longissimus dorsi* muscle heat-treated at four different temperatures: raw, 45, 60, and 70 °C (from bottom to top).

from glycine backbone and proline side chains. The bands at 1086 and 1036 cm^{-1} are due to carbohydrate residues. These characteristic absorption bands can be in general observed in IR spectra from collagen (*33, 34*) leading to the conclusion that the major bands in the connective tissue matrix are due to the protein collagen. Assignment of IR absorptions to precise constituents of connective tissue requires an understanding of the structure and function of this complex tissue. The major constituent of connective tissue is collagen as generally accepted and also obvious from the IR spectrum in **Figure 7**. This component is important since it contributes significantly to the toughness in mammalian muscle. Collagen occurs in several polymorphic forms, of which the most common type is type I. Collagen type I exists as a triple-stranded helix, containing two identical polypeptide chains and a third chain, which has a different amino acid sequence (*35*). This suprahelical structure is favored by the unique amino acid composition (25% proline/hydroxyproline and 33% glycine) and stabilized by numerous interstrand hydrogen bonds conferring remarkable mechanical properties to this protein.

As was found with the myofiber spectra, comparison of the connective tissue spectra obtained from different temperatures demonstrates that the major changes upon heat treatment occur in the amide I region. To resolve the overlapping amide I band components and hence the secondary structure of the connective tissue, again derivatization was applied.

The second derivatives of the same connective tissue spectra as in **Figure 7** are shown in **Figure 8** in the spectral region between 1750 and 1500 cm^{-1}. As compared to the second derivatives of the myofiber spectra (**Figure 3**), the second derivatives of the connective tissue spectra reveal less dramatic spectral alterations in the amide I region during the heat-induced denaturation. The following effects can be observed. With increasing temperature, a clear shift of the band at 1636 cm^{-1} toward lower frequencies, i.e., 1630 cm^{-1}, combined with a gain in band intensity, takes place. Simultaneously, the band at 1695 cm^{-1} develops also a higher band intensity with increasing temperature. As already stated, these bands are diagnostic for antiparallel β-sheets. Although collagen is mostly helical, it has to be taken into account that the connective tissue contains in addition other components, e.g., glycoproteins, which exhibit a different conformation. This might be mainly β-sheet structures as indicated by the two bands at 1630 and 1695 cm^{-1}, which

Denaturation Processes in Aged Beef Loin

J. Agric. Food Chem., Vol. 52, No. 12, 2004   **3925**

Figure 8. Normalized second derivatives of average spectra obtained from 90 single spectra of connective tissue from bovine *longissimus dorsi* muscle heat-treated at four different temperatures, i.e., raw, 45, 60, and 70 °C (from bottom to top) are displayed over the frequency range 1750–1500 cm^{-1} (amide I and II region). The SDs for the raw and the 70 °C heat-treated muscle are shown in the bottom.

are already present in the spectrum (black) of the raw *longissmus dorsi* sample in **Figure 8**. As a consequence, the distinct shift toward lower wavenumbers during the heating and the intensity increase, which can be observed for both bands, and the low frequency β-component at 1630 cm^{-1} and the high frequency β-component at 1695 cm^{-1} can be ascribed to an increasing transition dipole coupling due to a higher content in aggregated β-sheets structures. Furthermore, as is evident from **Figure 8**, the decrease of the content in α-helical structures upon heating is less pronounced than was found for the denaturation process in the myofiber proteins. This can be ascribed to the fact that the breakdown of the stable suprahelical structure of collagen takes place only at temperatures above 70 °C, resulting in conversion of the helical collagen structure to a more amorphous form, known as gelatin. Again, as was found with the myofiber spectra, the SDs of the connective tissue spectra of the 70 °C heat-treated sample are larger than for the raw sample (see bottom of **Figure 8**). However, the difference is not as dramatic as for the myofiber spectra, since collagen, the main component of the connective tissue, denatures completely only above 70 °C.

3.2.2. Spectral Alterations in the Chemical Images upon Heat Treatment. To visualize the spectral intensity in terms of total amount of biomass within the IR images, intensity plots of the EMSC parameter b_i, which corresponds to the multiplicative effect present in the spectra, are displayed in **Figure 9a–d**. Using the EMSC parameter b_i to visualize the total spectral intensity has the inherent advantage that the intensity plots are based on entire spectra instead of single bands, e.g., the amide I, resulting in a much more realistic concentration distribution. From the intensity plots in **Figure 9**, it is obvious that in general the absorbance values of myofibers are higher than absorbance of connective tissue, as indicated by the yellow or red color of the myofibrils, in contrast to the blue color of the connective tissue. Additionally, with increasing temperature and upon different shrinkage processes, the myofiber spectra gain significantly in intensity, whereas the intensity of the spectra recorded from the extra cellular space becomes gradually lower. However, this gain in intensity is not only due to the physical shrinkage of the myofibers, which is accompanied by a

Table 1. Assignment of Some Characteristic Bands in the IR Spectra of *Longissiumus dorsi* Muscle Tissue

spectral region/ frequency (cm^{-1})	assignment[a,b]
3050–2800	dominated by C–H strechting vibrations of fatty acids (mostly of membrane lipids)
2955	C–H str (asym) of –CH$_3$ in fatty acids
2930	C–H str (asym) of >CH$_2$
2918	C–H str (asym) of >CH$_2$ in fatty acids
2898	C–H str of C–H in methine groups
2870	C–H str (sym) of –CH$_3$
2850	C–H str (sym) of >CH$_2$ in fatty acids
1800–1500	dominated by absorption of proteins
1740	>C=O str of ester carbonyl of phospholipids
1715	>C=O str of carbonic acid
1680–1715	>C=O in nucleic acids
1695, 1685, 1675	amide I[c] band components resulting from antiparallel pleated sheets and β-turns of proteins
1655	amide I[c] of α-helical structures
1637	amide I[c] of β-pleated sheet structures
1550–1520	amide II[d]
1515	"tyrosine" band
1468	C–H def of >CH$_2$ groups of lipids, proteins, and nucleic acids
1400	C=O str (sym) of COO$^-$ groups
1310–1240	amide III band components of proteins
1250–1220	P=O str (asym) of >PO$_2^-$ phosphodiesters
1200–1000	C–O, C–C str, C–O–H, C–O–C def of carbohydrates
1090–1085	P=O str (sym) of >PO$_2^-$

[a] Peak frequencies have been deduced from the second derivatives and Fourier-deconvoluted spectra. [b] Str = stretching; def = deformation; sym = symmetric; and asym = antisymmetric. [c] Amide I band is a vibrational mode, which involves mainly C=O stretching vibrations. [d] Amide II band represents stretching of the C–N and in-plane bending of the N–H bonds.

substantial fluid loss, but also due to the molecular shrinkage of the myofibrillar proteins, i.e., the change in the conformation upon heating results in aggregation of the proteins that are much more dense than proteins in their native state.

Chemical images were reconstructed for all four heat-treated muscle samples of each of the four animals. The right side column of **Figure 10** shows the four chemical images obtained from the four different temperatures of one animal as an example. They were reassembled by using the I_{1630}/I_{1654} band ratio as a measure for the denaturation level. The black areas in the chemical images displayed in **Figure 10a–d** mark those spectra that have not passed the quality test (see section 2.2.3)) and were therefore not subjected to further evaluation.

Comparison of the four chemical images (see **Figure 10a–d**) shows that denaturation of the myofibrillar proteins was occurring at 45 °C, as indicated by the increase in light yellow color, whereas the connective tissue proteins show first signs of denaturation only at 60 °C. The image obtained from a raw *longissimus dorsi* sample proves that the proteins are still in their native conformation.

Figure 10b demonstrates that an initial stage of denaturation already takes place at 45 °C. The myofibers are not as compact as in **Figure 10a**, and gaps due to shrinkage processes are already clearly visible between the fibers. In addition, the chemical image shows that the structure of the outer part of the myofibers has started to change. These findings are in accordance with LF NMR (low field nuclear magnetic resoncance) measurements obtained during cooking of meat, where it was shown that the early phase of myosin denaturation starting at 40 °C causes small amounts of water to be squeezed out of the myofibrils into the intermyofibrillar space (*36*). This effect is even more pronounced when the lateral contraction of the

3926 *J. Agric. Food Chem.,* Vol. 52, No. 12, 2004

Kirschner et al.
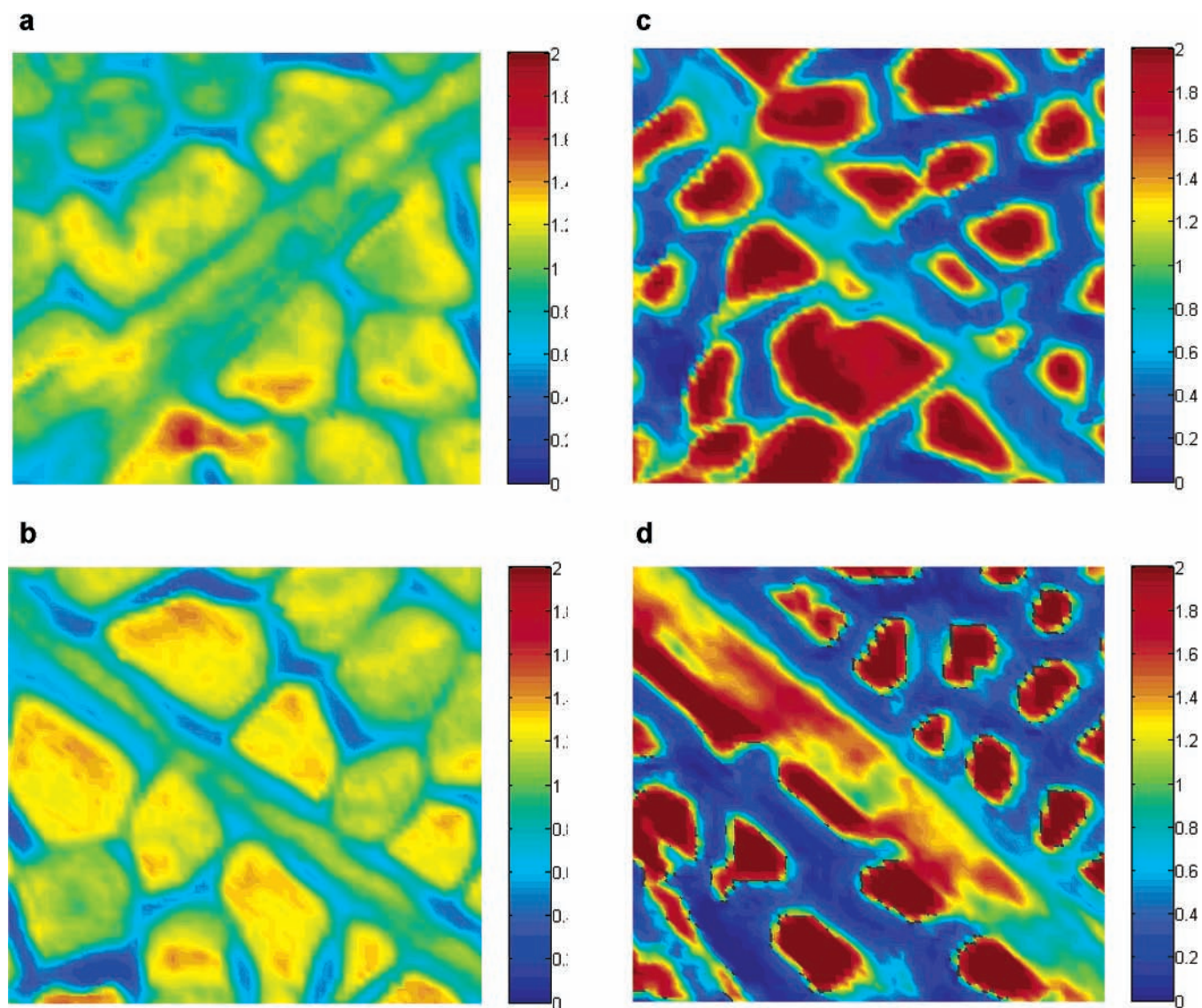
Figure 9. Intensity plots of the EMSC parameter b_i, which corresponds to the multiplicative effect, are displayed. The plots were obtained from sample 1 from the four different temperatures: raw, 45, 60, and 70 °C (from top to bottom). The multiplicative effect is due to differences in the amount of biomass present within the sample.

myofibrils occurs at about 45 °C. Although this aggregation of the denatured myofibrillar proteins, mainly myosin, results in shrinkage of the muscle fibers, the water/protein mixture is still retained within the endomysial sheath. This hypothesis is supported by the chemical image in **Figure 10b**, showing a higher denaturation level in the outer parts of the muscle fibers.

The chemical images at 60 and 70 °C, however, demonstrate a more dramatic change of both tissue structures. At 60 °C, a clear increase in the denaturation of the myofibers is visible as indicated by the yellow- and red-colored areas. Interestingly, the myofibers are obviously not homogeneously denatured, exhibiting a higher denaturation level in the outer part than in the inner part of the muscle fibers. This might be attributable to indirect effects of the collageneous endomysium and perimysium, which, due to shrinkage forces upon heating, may drive out denatured myofibrillar fluid from the muscle fibers resulting in highest denaturation in the outer parts of the myofibers (see **Figure 10c,d**). At 70 °C, it can be expected that the denatured myofibrillar fluid is to a large extent completely expelled from the myofibers due to heat-induced collagen contraction. Therefore, the myofibers in **Figure 10d** show a somewhat lower denaturation level as indicated by the mainly

green-colored fibers than the myofibers in **Figure 10c**. However, as already indicated in **Figure 9c,d**, the spectra recorded from the intermyofibrillar space exhibited such low spectral intensities that it was not possible to detect myofibrillar fluid in the intermyofibrillar space. In addition, upon heating at 70 °C, shrinkage of the myofibers becomes more apparent leading to clearly less structured fibers than at 60 °C. As expected from the gelatinization of collagen (collagen−gelatin transition), which takes place at temperatures above 70 °C, the connective tissue shows a lower denaturation level than the myofibers.

3.3. PLSR Results. PLSR was used to correlate the IR spectra to the temperatures used for the heat treatment. Additionally, jack-knifing was applied as a variable selection method to select the most significant variables (*37*). Jack-knifing is a variable selection method included in the Unscrambler software package (version 7.6; Camo ASA). It performs a significance test for all the wavenumbers of the IR spectra.

The root-mean-square error (RMSE) was a measure to assess the performance of the model. RMSE was calculated from a block-wise cross-validation as described previously (*38*), where all spectra referring to one animal were left out as one block.

Denaturation Processes in Aged Beef Loin

J. Agric. Food Chem., Vol. 52, No. 12, 2004   **3927**
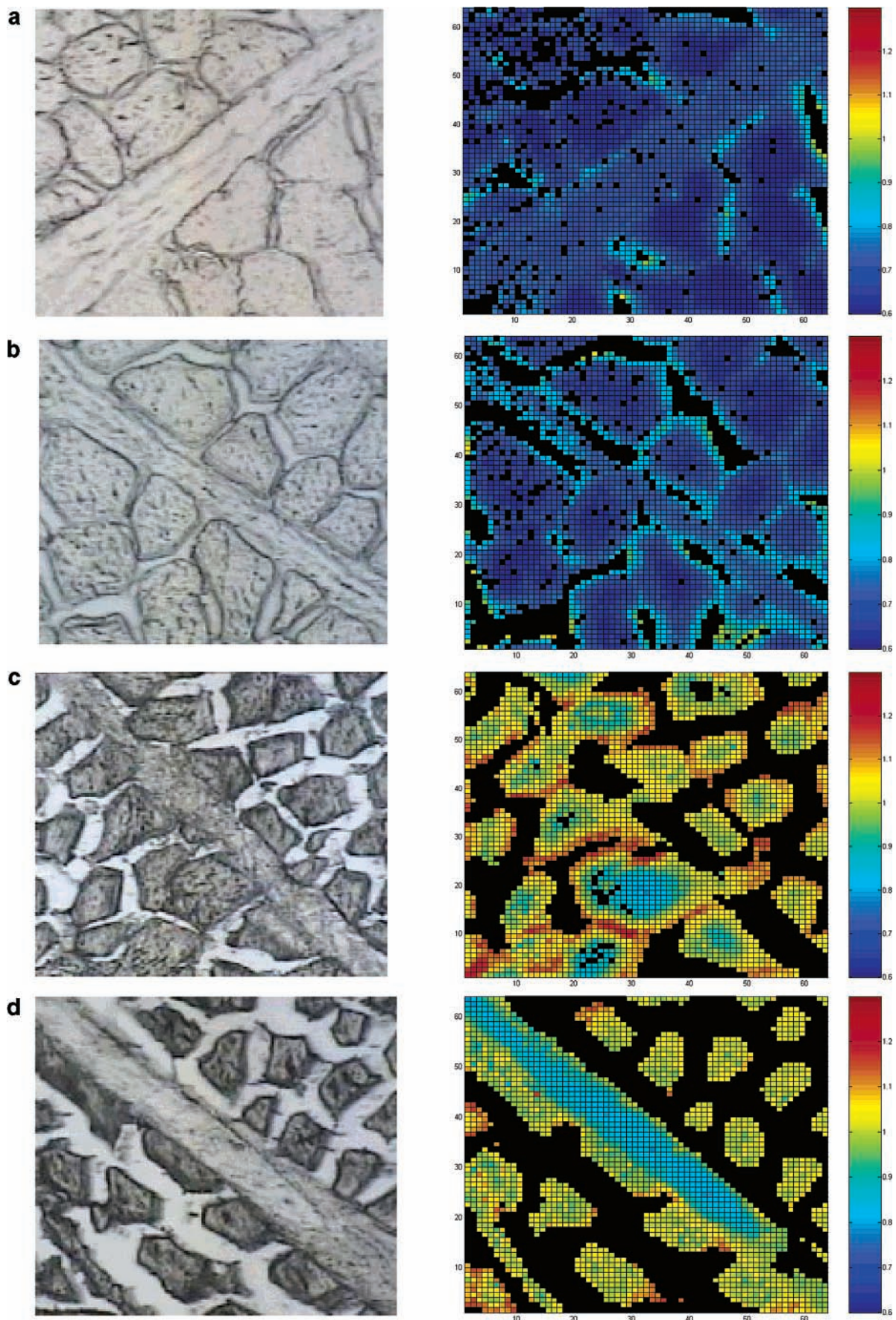
Figure 10. Chemical images of sample 1 obtained from four different temperatures: raw, 45, 60, and 70 °C (from top to bottom). Chemical images were reconstructed from the FPA images by using the I_{1630}/I_{1654} band ratio as a measure for the denaturation level. The scales on the right side of each image indicate the denaturation level. Corresponding photomicrographs of the IR images are displayed on the left side of each image. The black areas in the images indicate those spectra that did not pass the quality test.

3928 *J. Agric. Food Chem.,* Vol. 52, No. 12, 2004

Kirschner et al.

Table 2. Correlation Coefficients for the Differentiation between Denatured Meat Samples (raw, 45 °C, 60 °C and 70 °C All Samples Are from day 7) Based on PLS Regression Including Jack-knifing to Select the Most Significant Variables

spectral region (cm^{-1})	connective tissue	myofibers
1780–1000	0.84 (2)[a]	0.94 (3)
1780–1500	0.84 (2)	0.94 (3)
1700–1600	0.85 (2)	0.94 (3)
1500–1200	0.77 (4)	0.88 (3)
1200–1000	−0.18 (1)	0.81 (3)
1780–1000	0.85 (2, 112 sel. var.[b])	0.94 (3, 184 sel. var.)
1780–1500	0.86 (3, 46 sel.var.)	0.95 (4, 124 sel. var.)
1700–1600	0.85 (3, 21 sel.var.)	0.94 (2, 52 sel. var.)
1500–1200	0.79 (3, 38 sel.var.)	0.92 (5, 153 sel. var.)
1200–1000		0.82 (4, 81 sel. var.)

[a] Values in parentheses express the number of principal components required to reach the minimum RMSE. [b] Abbreviations: sel. var., selected variables that resulted from applying jack-knifing in order to choose the most significant variables.

The optimal number of components is found by calculating the minimum RMSE and checking if the change in RMSE for the preceding component was substantial (Camo AS, 1996). PLS regression was applied to all myofiber (80) and connective tissue (48) spectra. Prior to PLSR, the spectra were preprocessed by calculating the first derivatives and vector-normalizing them in the respective spectral region. **Table 2** shows the regression coefficients for the PLSR of the preprocessed FT-IR spectra and the different temperatures used for the heat treatment. For the connective tissue, five spectral outliers were identified and omitted from further analyses. All PLS regressions were performed using the following five spectral regions (see **Table 2**): 1780−1000, 1780−1500, 1700−1600, 1500−1200, and 1200−1000 cm^{-1}. This was done primarily to specifically investigate spectral ranges, which are dominated by certain components present in muscle tissue, such as proteins and polysaccharides, and also to reduce the dimensionality of the data. The numbers of principal components used for the PLSR regression are shown in parentheses. The lower the number of principal components required to build the model, the more stable and simpler the model becomes. The number of principal components is determined as described above. The best results were obtained for the protein-dominated spectral region from 1780 to 1500 cm^{-1} for both tissue structures, i.e., myofibers and connective tissue. Jack-knifing did not substantially improve the results. PLS regression based on the connective tissue spectra resulted in lower correlation coefficients than for the myofiber spectra. This might be attributed to the fact that the alterations in the myofiber spectra were much more pronounced than in the connective tissue spectra, since the denaturation temperature of collagen was not in the temperature range used for the heat treatment in this study. It should be noted that this approach is based on a linear dependency between temperature and spectral information. However, the objective was to identify the spectral region reflecting the denaturation process and not to optimize correlation coefficients.

CONCLUSIONS

In this study, beef *longissimus dorsi* muscles from four different animals were heat-treated at four different temperatures, i.e., raw, 45, 60, and 70 °C. FT-IR microspectroscopy was used as a spatially resolved method to monitor the changes in the meat caused by cooking. The results illustrate that FT-IR microspectroscopy, employing both a single element and a FPA detector, can be used to detect the heat-induced denaturation processes in meat very precisely. By using FPA imaging, it was possible to monitor the heat denaturation of the two major meat components, i.e., myofibrillar and connective tissue proteins, spatially resolved. Furthermore, evaluation of average spectra of these two major meat structures obtained either from single element measurements or from the complex FPA images showed very distinct conformational changes in the amide I region indicating an increase in β-sheet and a decrease in α-helical structures at higher temperatures. These major conformational changes, which were much more pronounced for the myofibers than for the connective tissue, could be correlated to the denaturation of the major meat proteins, e.g., actin, myosin, and collagen. In addition, using PCA as a multivariate data analysis revealed that the spectra obtained from the myofibers at 70 °C showed the highest variance indicating a transition temperature, which is in agreement with the denaturation temperature from actin, ranging from 65 to 73 °C. For the evaluation of the complex FPA images, in-house developed software was presented. It can be concluded that FT-IR microspectroscopy may provide a useful tool for monitoring thermal processing of meat.

LITERATURE CITED

(1) Palka, K.; Daun, H. Changes in texture, cooking losses, and myofibrillar structure of bovine M. semitendinosus during heating. *Meat Sci.* **1999**, *51*, 237−243.

(2) Harper, G. S. Trends in skeletal muscle biololgy and the understanding of toughness in beef. *Aust. J. Agric. Res.* **1999**, *50*, 1105−1129.

(3) Nishimura, T., et al. Changes in mechanical strength of intramuscular connective tissue during postmortem aging of beef. *J. Anim. Sci.* **1998**, *76*, 528−532.

(4) Akahane, T., et al. Differential scanning calorimetric studies on thermal behaviour of myofibrillar proteins. *Bull. Jpn. Soc. Sci. Fish.* **1985**, *51* (11), 1841−1846.

(5) Xiong, Y. L.; Brekke, C. J.; Leung, H. K. Thermal denaturation of muscle proteins from different species and muscle types as studied by differential scanning calorimetry. *Can. Inst. Food Sci. Technol. J.* **1987**, *20* (5), 357−362.

(6) Stabursvik, E.; Fretheim, K.; Fröystein, T. Myosin denaturation in pale, soft, and exudative (PSE) porcine muscle tissue as studied by differential scanning calorimetry. *J. Sci. Food Agric.* **1984**, *35*, 240−244.

(7) Wright, D. J.; Wildling, P. Differential scanning calorimetric study of muscle and its proteins: myosin and its subfragments. *J. Sci. Food Agric.* **1984**, *35*, 357−372.

(8) Palka, K. The influence of post-mortem aging and roasting on the microastructure, texture and collagen solubility of bovine semitendinosus muscle. *Meat Sci.* **2003**, *64*, 191−198.

(9) Messerschmidt, R. G.; Harthcock, R. G. *Infrared Microspectroscopy: Theory and Applications*; Messerschmidt, R. G., Harthcock, R. G., Eds.; Marcel Dekker: New York and Basel, 1988.

(10) Lewis, E. N., et al. Fourier transform spectroscopic imaging using an infrared focal-plane array detector. *Anal. Chem.* **1995**, *67*, 3377−3381.

(11) Haka, A. S.; Levin, I. W.; Lewis, E. N. Uncooled barium strontium titanium focal plane array detection for mid-infrared Fourier transform spectroscopic imaging. *Appl. Spectrosc.* **2000**, *54* (5), 753.

(12) Lasch, P., et al. Characterization of colorectal adenocarcinoma sections by spatially resolved FT-IR Microspectroscopy. *Appl. Spectrosc.* **2002**, *56* (1), 1−9.

(13) Kneipp, J., et al. Molecular changes of preclinical scrapie can be detected by infrared spectroscopy. *J. Neurosci.* **2002**, *22* (8), 2989−2997.

(14) Marcott, C., et al. FT-IR spectroscopic imaging of wheat kernels using a Mercury−Cadmium−Telluride focal-plane array detector. *Vib. Spectrosc.* **1999**, *19*, 123−129.

(15) Budevska, B. O.; Sum, S. T.; Jones, T. J. Application of multivariate curve resolution for analysis of FT-IR microspectroscopic images of in situ plant tissue. *Appl. Spectrosc.* **2003**, *57* (2), 124−131.

(16) Hildrum, K. I., et al. Prediction of sensory characteristics of beef by near-infrared spectroscopy. *Meat Sci.* **1994**, *38*, 67−80.

(17) Gronholz, J.; Herres, W. Understanding FT-IR data processing. *Instrum. Comput.* **1985**, *3*, 10−19.

(18) Helm, D.; Labischinski, H.; Naumann, D. Elaboration of a procedure for identification of bacteria using Fourier Transform IR spectral libraries: a stepwise correlation approach. *J. Microbiol. Methods* **1991**, *14*, 127−142.

(19) Bruker. *Opus I. R. Handbook*; Bruker Optics: Karlsruhe, Germany, 1991.

(20) Martens, H.; Nielsen, J. P.; Engelsen, S. B. Light scattering and light absorbance separated by extended multiplicative signal correction. Application to near-infrared transmission analysis of powder mixtures. *Anal. Chem.* **2003**, *75* (3), 394−404.

(21) Fabian, H.; Mäntele, W. Infrared Spectroscopy of Proteins. In *Handbook of Vibrational Spectroscopy*; Chalmers, J. M., Griffiths, P. R., Eds.; John Wiley & Sons Ltd.: Chichester, 2002; pp 3399−3425.

(22) Krimm, S.; Bandekar, J. Vibrational Spectroscopy and Conformation of Peptides, Polypeptides and Proteins. *Adv. Protein Chem.* **1986**, *38*, 181−364.

(23) Jackson, M.; Mantsch, H. H. The use and misuse of FTIR spectroscopy in the determination of protein structure. *Crit. Rev. Biochem. Mol. Biol.* **1995**, *30* (2), 95−120.

(24) Martens, H.; Næs, T. *Multivariate Calibration*; John Wiley & Sons: Chichester, 1989.

(25) Ouali, A. Meat tenderization: Possible causes and mechanisms. *J. Muscle Fd.* **1990**, *1*, 129−165.

(26) Ofstad, R., et al. Liquid loss as effected by post-mortem ultrastructural changes in fish muscle; Cod (Gadus morhua L.) and Salmon (Salmo salar). *J. Sci. Food Agric.* **1996**, *71*, 310−312.

(27) Christensen, M.; Purslow, P. P.; Larsen, L. M. The effect of cooking temperature on mechanical properties of whole meat, single muscle fibres and perimysial connective tissue. *Meat Sci.* **2000**, *55*, 301−307.

(28) Fabian, H.; Schultz, C. P. Fourier Transform Infrared Spectroscopy in Peptide and Protein Analysis. In *Encyclopedia of Analytical Chemistry*; Mayers, R. A., Ed.; John Wiley & Sons Ltd.: Chichester, 2000; pp 5779−5803.

(29) Moore, W. H.; Krimm, S. Transition Dipole Coupling in Amide I Modes of β-Polypeptides. *Proc. Natl. Acad. Sci.* **1975**, *72* (12), 4933−4935.

(30) Moore, W. H.; Krimm, S. Vibrational Analysis of Peptides, Polypeptides and Proteins. II. Poly(L-alanine) and beta-Poly(L-alanylglycine). *Biopolymers* **1976**, *15*, 2465−2483.

(31) Manning, C. J.; Griffiths, P. R. Noise sources in step-scan FT-IR Spectrometry. *Appl. Spectrosc.* **1997**, *51* (8), 1092−1101.

(32) Bhargava, R.; Levin, I. W. Fourier transform infrared imaging: theory and practice. *Anal. Chem.* **2001**, *73*, 5157−5167.

(33) Dukor, R. K. Vibrational spectroscopy in the detection of cancer. In *Encyclopedia of Analytical Chemistry*; Meyers, R. A., Ed.; John Wiley & Sons Ltd.: Chichester, 2000; pp 3335−3361.

(34) Jackson, M., et al. Beware of connective tissue proteins: assignment and implications of collagen absorptions in infrared spectra of human tissues. *Biochim. Biophys. Acta* **1995**, *1270* (1), 1−6.

(35) Sims, T. J.; Bailey, A. J. Connective tissue. In *Developments in Meat Science*; Lawrie, R., Ed.; Applied Science: London, 1981; pp 29−59.

(36) Micklander, E., et al. NMR-cooking: monitoring the changes in meat during cooking by low-field ¹H NMR. *Trends Food Sci. Technol.* **2002**, *13*, 341−346.

(37) Westad, F.; Martens, H. Variable selection in near-infrared spectroscopy based on significance testing in partial least squares regression. *J. Near Infrared Spectrosc.* **2000**, *8*, 117−124.

(38) Stone, M. Cross-validatory choice and assessment of statistical predictions. *J. R. Stat. Soc. B* **1974**, 111−133.